Geotechnical Aspects of Underground Construction in Soft Ground, Kastner, Emeriault, Dias, Guilloux (eds)
 ISBN 2-9510416-3-2

Lateral Earth Pressures induced by Wall Movements in Centrifuge Tests

Y. Toyosawa, N. Horii, S. Tamate
Independent Administrative Institution, National Institute of Industrial Safety, Tokyo, Japan
N. Suemasa, T. Katada, T. Ichikawa
Musashi Institute of Technology, Tokyo, Japan

ABSTRACT: Interactions between the movement of retaining walls, deformation of soil, generation of lateral earth pressures, and the behavior that leads to collapse are very complicated. To clarify the relevance of earth pressures to the wall movement pattern or rupture mechanism behind the wall, the newly developed movable earth support system, which represents various movements of a wall at a centrifuge acceleration of 50g, was used for measuring the lateral pressure on a retaining wall. Test results imply that: (1) Lateral earth pressure decreased with wall movement on the active side; however, the redistribution of earth pressure and the development of strains varied depending on the mode of wall movement. (2) Until the movement of the wall reached X/L =0.01, the activated area propagated behind the wall in a wedge shape. (3) For rotation about the top, translation and center swelling cases, it is assumed that the arching action has a significant effect on the redistribution of earth pressure. (4) In the case of rotation about the base, it is supposed that the active state started from around X/L=0.01.

1 INTRODUCTION

To prevent the accidental collapse of earth supports in construction work, knowledge about collapse mechanisms, collapse precursors, and so forth are needed. However, the interaction between the generation of lateral earth pressures, deformation of soil, movement of retaining walls and the behavior that leads to collapse are very complicated. Therefore, it is difficult to predict accurately whether the observed movement at a construction site will result in a collapse, or whether the movement will stop.

Further research is required to take account of wall movement, deformation in the soil, and the phenomena that lead to collapse. This research investigates the interaction between the generation of earth pressures and soil deformation due to wall movement. Centrifuge experiments were carried out using the newly developed movable earth support equipment, which controls the wall movements with high precision in a 50g centrifugal field. For the analysis of soil deformation, an image-processing system was utilized.

2 MOVABLE EARTH SUPPORT EQUIPMENT FOR CENTRIFUGE MODEL EXPERIMENT

The movable earth support equipment, which was developed for centrifuge model experiments, is shown in Figure 1. This equipment reproduces various movement states of a retaining wall, which is divided into five boards, by moving the five boards independently in the horizontal direction. As shown in Figure 1, the five boards made of aluminum (height of 40 mm, width of 99 mm) are attached at the end of each strut.

A load cell (a gate type load cell, maximum allowable load of 400 N) is set just behind each divided board, and the axis load acting on each divided board can be measured.

The inside dimensions of the model strongbox are: length 350 mm, height 270 mm, and width 100 mm. This movable earth support equipment can be set from the side of the strongbox.

The moving direction and speed of each divided board can be controlled independently by a PC in a control room through RS-232C (through a slip ring). Five 100V/15W reversible motors are used. The speed control range is 1-18 mm/min (when gears are changed, the speed control range is 0.1-1.8 mm/min), and the maximum movable distance is 4 cm.

For verification of these load cells, a specific tool, which reproduces pull and compression loads at 50g by using weights, is used. Furthermore for verification, a rubber back filled with water was installed in the strongbox, and the horizontal water pressure was measured at 50g.

3 MONITOR AND IMAGE-PROCESSING SYSTEM

Figure 2 shows a plane view of the monitoring system of the model ground. An on-board 400,000-pixel CCD camera and lights are set in front of the model ground. Image data is monitored in the control room and recorded on a DV-video tape recorder. Image data is transmitted through a television aerial receiver and transmitter that are mounted at the center of the centrifuge. Frames of 640×480 pixels are used.

Displacement is one of the most significant parameters to be measured in centrifuge tests. The most simple but effective method of observing the progress of a test in real-time is by subtracting images of two different stages, which enables visualization of how the deformation proceeds.

4 MODEL PREPARATION AND TEST PROCEDURE

Dry Toyoura sand was poured into the strongbox by the falling method, and the model ground of 180 mm height and 70% dry density was prepared. Thin layers with colored sand were inserted every 2 cm in height for cases 1 to 7. For cases 8 to 11, the inside of the strongbox (sidewalls) are lubricated with grease and a thin rubber membrane with a thickness of 0.02mm is added. Then the friction between the sand and sidewalls decreased 15 degrees to almost 1 degree.

A thin aluminum plate with a relatively smooth surface (friction angle between aluminum and sand is about 24 degrees) and thickness of 0.2 mm was set between the sand and wall for Cases 1 to 3. For Cases 4 to 7, the aluminum plates were pasted with sand (rough surface, friction angle is 36 degrees).

Four wall movement modes were used for the ex-

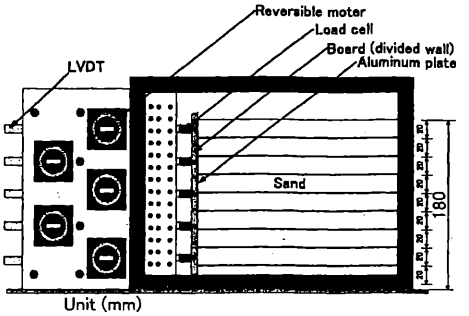

Figure 1 Movable earth support equipment

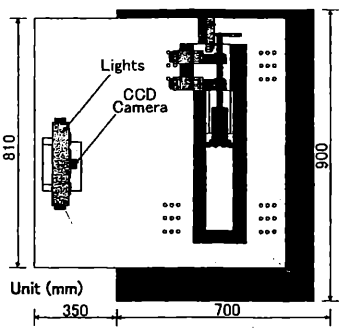

Figure 2 Plain view of monitor system

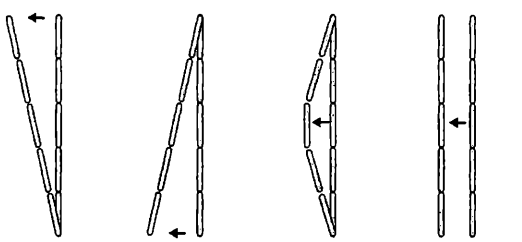

Figure 3 Wall movement modes.

Table 1 Test conditions.

Case	Kind of soil	Relative density (Dr)	Model ground height	Model wall surface	Friction between sand and side walls	Mode of wall movement
1	Toyoura sand	70%	180mm	Aluminum	Non-lubricated	Rotation about base
2						Rotation about top
3						Swelling of center (rotation about top and base)
4				Rough (sand surface)		Rotation about base
5						Rotation about top
6						Swelling of center (rotation about top and base)
7						Translation
8					Lubricated	Rotation about base
9						Rotation about top
10						Swelling of center (rotation about top and base)
11						translation

periments: (1) rotation about base, (2) rotation about top, (3) central part swelling, and (4) translation (displacement toward the active side, with the wall kept vertical), as shown in Figure 3 at 50g. Lateral earth pressures (acting on each divided board) and displacement of the board were measured. Table 1 shows the conditions of these tests.

5 TEST RESULTS AND DISCUSSIONS

5.1 *Image data analysis*

Figure 4 and Figure 5 show the sequence of deformation in Case 9 induced by rotation of the retaining wall about the top (as illustrated in Figure 3-(2)) and in Case 10 induced by swelling of the retaining wall (as illustrated in Figure 3-(3)) respectively. The value of X/L (X: distance of horizontal movement of 3rd axis, L: height of model ground at 3rd axis.) in each figure indicates the inclination of the retaining wall.

A rupture line appeared when X/L reached around 0.02 and the deformation progressed along the rupture surface.

Figure 6 shows the deformation area visualized by using image processing when (1) X/L=0.00 to 0.01, (2) X/L=0.01 to 0.02, and (3) X/L=0.02 to 0.04. Until X/L reached 0.01, a wedge-shaped deformation area developed behind the wall as shown in Figure 6 (X/L=0.00 to 0.01). After a rupture surface appeared, the deformation area was limited within the area enclosed by the rupture surface and wall.

5.2 *Lateral earth pressures and wall movements*

The lateral earth pressure decreased with the wall movement on the active side in every test, however, the redistribution of earth pressure varied depending on the mode of wall movement.

The distribution of lateral earth pressure on the wall at X/L=0.02 in Case 1, Case 4, and Case 8 (the wall rotated about the base) became similar to Rankine's active earth pressure.

Figure 7 shows the distribution of lateral earth pressures on the wall at X/L=0.02 in Case 5, Case 9, and the calculated earth pressure according to the method that is illustrated in 5.4. The measured earth pressure is close to Jaky's earth pressure at rest at the upper wall and smaller than Rankine's earth pressure at the lower part of the wall when the wall is rotated about the top. It is assumed that when the wall movement is small in the upper part of the wall, the soil behind the upper part has not reached the limiting state condition; therefore, the value of earth pressure of the upper part is similar to the earth pressure at rest while the wall movement in the lower part would be sufficient to become an active state for the sand. Moreover, the vertical stress would reduce

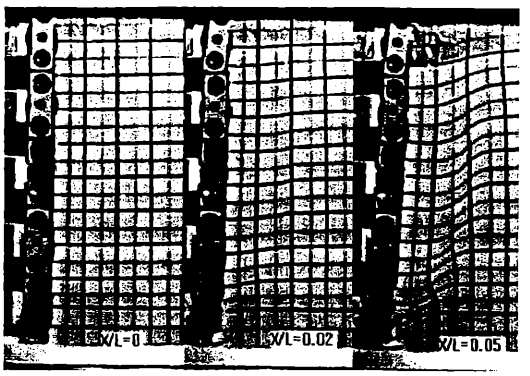

Figure 4 Sequence of deformation in Case 9 (rotation about top).

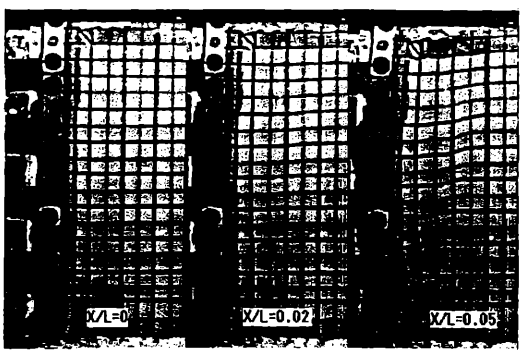

Figure 5 Sequence of deformation in Case 10 (swelling of center (rotation about top and base).

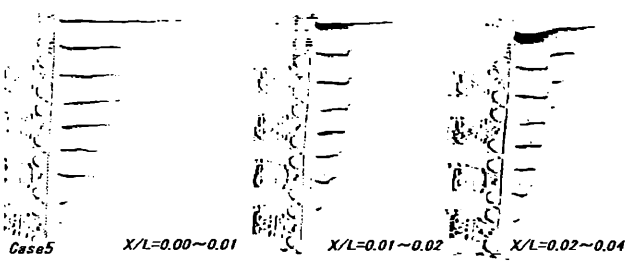

Figure 6 Visualized deformation area in Case5 (rotation about top).

in the lower area because of the arching action that occurred at the upper area behind the wall.

Comparing Case 2 and Case 5, both cases having the same rotational movement about the base, but the roughness (friction) of the wall surface is different (Case 2 is aluminum, Case 5 is sand pasted on aluminum). The lateral earth pressures in Case 5,

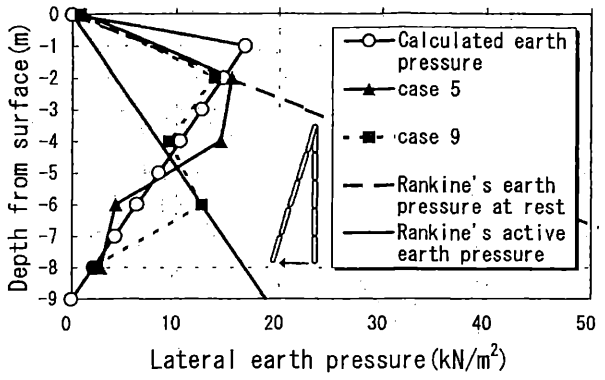

Figure 7 Distribution of lateral earth pressures on wall (X/L=0.02) (rotation about top, Fig3-(2)).

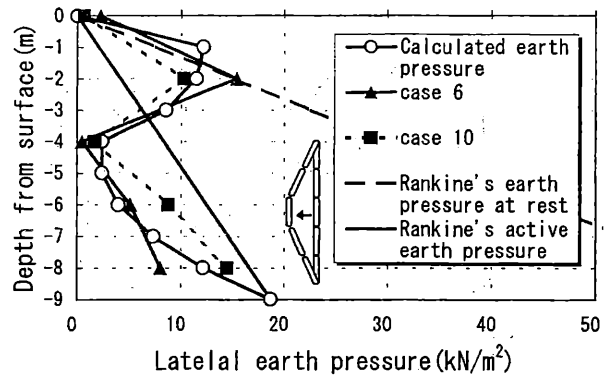

Figure 8 Distribution of lateral earth pressures on wall (X/L=0.02) (center swelling, Figure 3-(3)).

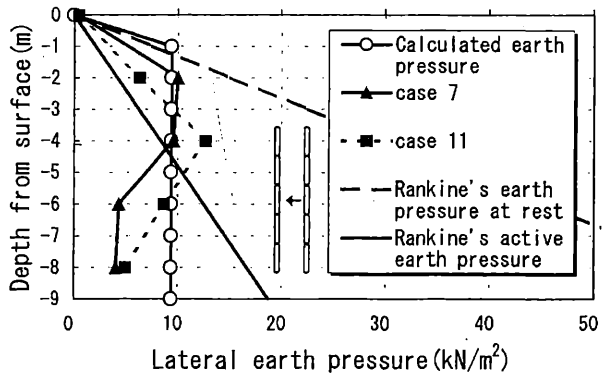

Figure 9 Distribution of lateral earth pressures on wall (X/L=0.02) (translation, Fig3-(4)).

compared to Case 2, are larger at the upper part of the wall and smaller at the lower part of the wall. This can be explained by the larger arching action that occurred in Case 5 than in Case 2.

Figure 8 indicates the distribution of the lateral earth pressure on the wall in Case 6 and Case 10 (rotation about top and base, central part of wall swelling) at X/L=0.02. The lateral earth pressure on the upper part of the wall is close to the earth pressure at rest and the lateral earth pressure on the lower part of the wall is smaller than Rankine's active earth pressure. When the movement of the wall is too small to reach an active state, it is supposed that the arching action works at the upper area, consequently the earth pressure becomes almost the same as the earth pressure at rest and the vertical stress is decreased by the arching action, hence the earth pressure on the lower wall is smaller than Rankine's active earth pressure even though the wall movement is large enough to reach an active state.

Figure 9 shows the lateral earth pressure distribution on the wall at X/L=0.02 in Case 7 and Case 11 (translation movement as shown in Figure 3-(4)). The lateral earth pressure on the upper part of the wall is close to the earth pressure at rest and the lateral earth pressure on the lower part of the wall is smaller than Rankine's active earth pressure.

In every case, the distribution of lateral earth pressure becomes close to the distribution of Rankine's active earth pressure when the wall movement is sufficiently large at X/L=0.04. This can be explained by the reduction of arching action and redistribution of earth pressure.

The total lateral earth pressure (summation of 5 boards) with the wall movement decreased immediately at the initial movement of the wall and then became constant. Regarding wall movement with rotation about the base, it is said that the soil becomes active at around X/L=0.001 by Terzaghi, and becomes active at X/L=0.02 to 0.04 by Ishihara. In our experiments, it is supposed that the active state started from around X/L=0.01.

5.3 *Effect of lubrication of strongbox's sidewalls*

The sand and sidewalls were lubricated with grease and a rubber membrane was applied to reduce the friction between the sand and sidewalls for Cases 8 to 11. As the result of the reduction of friction, the arching action was reduced. Consequently, the earth pressure decreased at the upper part, and in contrast the earth pressure increased at lower part. The arching action, which was reproduced by friction between the sand and sidewalls, affected the distribution of earth pressure significantly.

Table 2 indicates the total earth pressures in Cases 4 to 11 at X/L=0.02 and increments of the total earth pressures, which represents the difference between the lubricated cases and non-lubricated cases. Because of the lubrication, 7 to 10 kN/m^2 (20-40%) of the total earth pressure was increased.

An increment of the earth pressure in Cases 5 and 9 induced by rotation about the top was smaller than the earth pressure induced by the other wall movements.

Table2 Total lateral earth pressures in the active state

Friction between sand and sidewalls / Wall movement	Non-lubricated (kN/m^2)	Lubricated with membrane and grease (kN/m^2)	Increment of total earth pressure (kN/m^2)
Rotation about base	21.43 (case4)	30.96 (case8)	9.53
Rotation about top	37.91 (case5)	38.66 (case9)	0.75
Swelling of center (rotation about top and base)	30.13 (case6)	36.70 (case10)	6.57
Translation	28.40 (case7)	38.52 (case11)	10.12

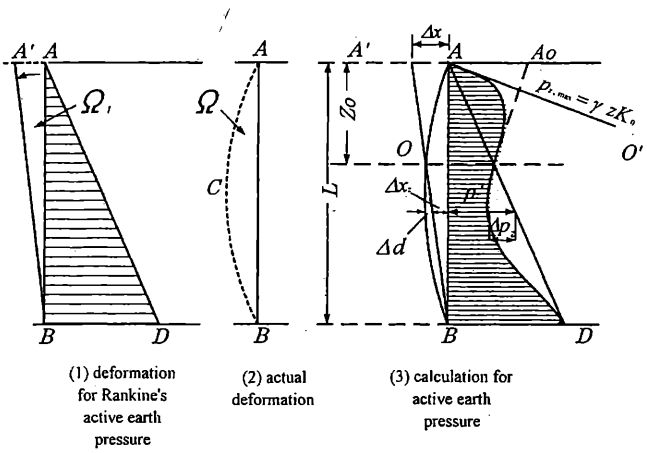

Figure 10 Calculation method for active earth pressure.

To reduce the friction, the usage of grease and a rubber membrane is effective. It can reduce the friction angle from 15 to 1 degrees.

5.4 *Calculated lateral earth pressures*

The calculated earth pressures are shown in figures 7, 8 and 9 respectively. The calculated values are almost the same as the measured earth pressures.

This calculation method is based on the following assumptions.

(1) The total earth pressure maintains the constant condition regardless of the amount of movement of the retaining wall, and is equal to the total active earth pressure in a limiting state condition.

(2) An earth pressure distribution becomes a triangle distribution as Rankine's active earth pressure in the case where the retaining wall rotates about base and ground moves to an active side.

The retaining wall changes like ACB, which is expressed with Ω in Figure 10-(2) when the earth pressure acts on retaining wall AB.

The area of triangle distribution of ABA' with an equal area is expressed with Ω_1, then the amount of movement of the upper end of the retaining wall is expressed with the following formula.

$$\overline{AA'} = \Delta x = \frac{2\Omega_1}{H} \tag{1}$$

Where $\Omega_1 = \Omega$,

The earth pressure (p_z) obtained from the above assumptions expressed as,

$$p_z = p'_z - \Delta p_z \tag{2}$$

$$p_z = nz + m(H - z) - \alpha f \tag{3}$$

Where,

$$n = K_A \cdot \gamma$$

$$m = \frac{K_A \cdot \gamma \cdot z_o}{H - z_o} = \frac{nz_o}{H - z_o}$$

$$\alpha = K_A \cdot \gamma \cdot z_o \cdot \frac{H}{\Delta x(H - z_o)} = \frac{mH}{\Delta x}$$

$$\Delta x = \frac{2\Omega}{H}$$

In the case for $z < z_o$,

$$f = \Delta x_z - \Delta d = \frac{\Delta x}{H}(H - z) - \Delta d \tag{4a}$$

for $z > z_o$,

$$f = \Delta x_z + \Delta d = \frac{\Delta x}{H}(H - z) + \Delta d \tag{4b}$$

5.5 *Development of displacements and strains*

Figure 11 shows the displacements of the model ground in Cases 8 and 10. These displacements developed mainly in the limited area surrounding within the failure line and the wall, as the wall movement progressed.

Figures 12 and 13 show the principal strains (ε_1, ε_3) that were calculated from the displacements in each stage. For the calculation, pictures taken by CCD camera with 0.4 megapixels were used. The failure line appeared when the maximum shear strains reached around 10% in the area the strains developed.

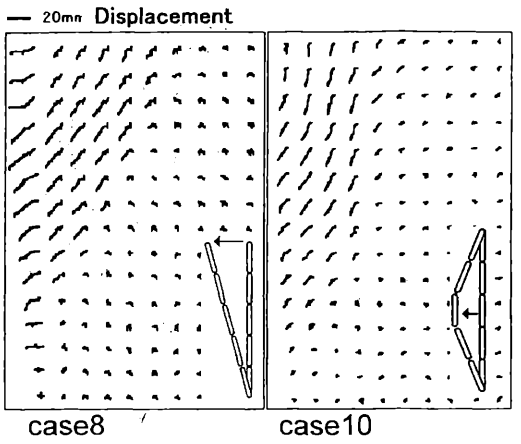

Figure 11 Displacements of model grounds in case8 and case10 (X/L=0~0.08).

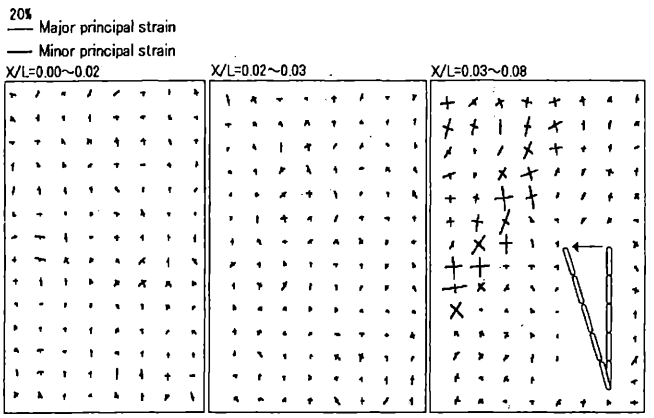

Figure 12 Principal strains (case8).

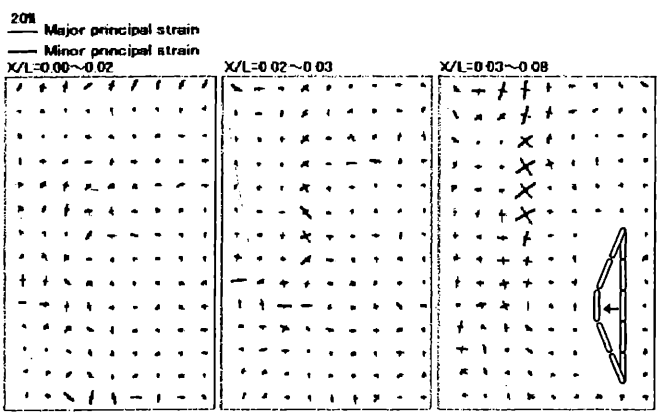

Figure 13 Principal strains (case10).

6 CONCLUSION

To clarify the relevance of earth pressure on the wall movement pattern or rupture mechanism behind the wall, the newly developed movable earth support system, which represents various movements of the wall in the field of 50g, was used for measuring the lateral pressure on the retaining wall in sand model ground. The following conclusions were obtained.

(1) Lateral earth pressure decreased with wall movement on the active side in every test, however, the redistribution of earth pressure, displacement of model ground and the development of strains varied depending on the mode of wall movement.

(2) Until the movement of the wall reached X/L=0.01, the activated area propagated behind the wall in a wedge shape. After the rupture surface appeared (analyzed by image processing), the deformation area was limited within the rupture surface and wall.

(3) For rotation about the top, translation and center swelling cases, lateral earth pressure on the upper part of the wall was close to the line of earth pressure at rest and the lateral earth pressure on the lower part of the wall was smaller than Rankine's active earth pressure at around X/L=0.02, so it is assumed that the arching action have a significant effect on the redistribution of earth pressure.

(4) In the case of rotation about the base, it is supposed that the active state started from around X/L=0.01.

(5) The calculated earth pressures are almost same as measured earth pressures.

REFERENCES

Chang, M.F. 1997. Lateral earth pressures behind rotating walls, *Can Geotech Journal* 34(4): 498-509.

Dubrova, G.A. 1963. *Interaction between soils and structures.* Moscow: Rechnoy Transport.

Fang, Y.S. & Ishibashi, I. 1986. Static earth pressures with various wall movements. *Journal of Geotechnical Engineering, ASCE* 112(3): 317-333.

Fang, Y.S., Cheng, F.P., Chen, R.C. & Fan, C.C. 1993. Earth pressures under general wall movements. *Journal of Geotechnical Engineering, ASCE* 24(2): 113-131.

Ishihara, K., 1988. *Soil mechanics.* Tokyo, Maruzen.

Matsuo, M., Kenmochi, S., & Yagi ,H. 1978. Experimental study on earth pressure of retaining walls by field tests. *Soils and Foundations* 18(3): 27-41.

Matsuzawa, H. & Hararika, H. 1996. Analyses of active earth pressure against rigid retaining walls subjected to different modes of movement. *Soils and Foundations* 36(3): 51-65.

Nakai, T. 1985. Finite element computations for active and passive earth pressure problems of retaining wall. *Soils and Foundations* 25(3): 98-112.

Sherif, M.A., Ishibashi, I. & Lee, C.D. 1982. Earth pressures against rigid retaining walls. *Journal of Geotechnical Engineering, ASCE*108(5): 679-695.

Sherif, M.A., Fang, Y.S. & Sherif, R.I. 1984. K_A and K_O behind rotating and non-yielding walls. *Journal of Geotechnical Engineering, ASCE*110(1): 41-56.

Taylor, D.W. 1941. Abstracts of selected theses in soil mechanics. *Department of Civil Engineering, Massachusetts Institute of Technology, Cambridge, Publication Series 79.*

Terzaghi, K. 1934. Large retaining wall tests I . Pressure in dry sand. *Engineering News Record, February* : 136-140.

Terzaghi, K. 1936. Distribution of lateral pressure on sand on the timbering of cuts. *Proceedings of 1st International Conference on Soil Mechanics and Foundation Engineering, Cambridge* 1: 211-215.

Terzaghi, K. 1941. General wedge theory of earth pressure. *ASCE Transactions* 106: 68-97.